Clays and Clay Minerals, Vol. 63, No. 3, 222–234, 2015.

CERAMIC MEMBRANES PREPARED FROM A SILICATE AND CLAY-MINERAL MIXTURE FOR TREATMENT OF OILY WASTEWATER

JUNG-HYE EOM[1], HEE-JONG YEOM[1], YOUNG-WOOK KIM[1,*], AND IN-HYUCK SONG[2]

[1] Functional Ceramics Laboratory, Department of Materials Science and Engineering, The University of Seoul, 163 Seoulsiripdae-ro, Dongdaemun-gu, Seoul 130-743, Korea

[2] Engineering Ceramics Group, Korea Institute of Materials Science, 531 Changwondaero, Changwon, Gyeongnam 641-831, Korea

Abstract—The application of ceramic membranes is limited by the high cost of raw materials and the sintering process at high temperatures. To overcome these drawbacks, the present study investigated both the preparation of ceramic membranes using cost-effective raw materials and the possibility of recycling the membranes for the treatment of oily wastewater. Ceramic membranes with a pore size of 0.29−0.67 μm were prepared successfully at temperatures as low as 1000−1100ºC by a simple pressing route using low-cost base materials including diatomite, kaolin, bentonite, talc, sodium borate, and barium carbonate. The typical steady-state flux, fouling resistance, and oil-rejection rate of the low-cost virgin membranes sintered at 1000ºC were 2.5×10^{-5} $m^3m^{-2}s^{-1}$ at 303 kPa, 63.5%, and 84.1%, respectively, with a feed oil concentration of 600 mg/L. A simple burn-out process of the used membranes at 600ºC in air resulted in >95% recovery of the specific surface area (SSA) of the virgin membranes, a significantly increased steady-state flux, decreased fouling resistance, and increased oil-rejection rate. The typical steady-state flux, fouling resistance, and oil-rejection rate of the low-cost ceramic membrane sintered at 1000ºC and subsequently heat treated at 600ºC for 1 h in air after the first filtration were 5.4×10^{-5} $m^3m^{-2}s^{-1}$ at 303 kPa, 27.1%, and 92.9%, respectively, with a feed oil concentration of 600 mg/L. The present results suggest that the low-cost ceramic membranes used for oily wastewater filtration can be recycled by simple heat-treatment at 600ºC in air. As the fouling resistance of the low-cost ceramic membranes decreased with a decrease in pore size, the preferred pore size of the membranes for oily wastewater filtration is <0.4 μm.

Key Words—Membrane, Oil-Water Emulsion, Processing, Recycling, Rejection Rate.

INTRODUCTION

Oily wastewater emulsions, which are difficult to treat, are one of the main industrial pollutants emitted into aquatic environments. The steel, metallurgical, petrochemical, transportation, textile, and oil-refinery industries produce oily wastewater emulsions in the concentration range of 50−1000 mg/L (Mueller *et al.*, 1997; Mohammadi *et al.*, 2004; Ezzati *et al.*, 2005; Zhang *et al.*, 2010; Vasanth *et al.*, 2013). This hazardous waste has to be treated to meet an acceptable discharge limit before it can be released into seas, lakes, or rivers. Conventional approaches to treat oily wastewater include coagulation/flocculation, air flotation, chemical de-emulsification followed by gravity settling, and ultrasonic separation (Cheryan and Rajagopalan, 1998; Kumara and Roy, 2008; Zhang *et al.*, 2010; Hajasgarkhani *et al.*, 2013). These methods have disadvantages such as low efficiency, high operating cost, and recontamination problems, however. Furthermore, they are not effective for the treatment of stable emulsions with low oil concentration (Chen *et al.*, 2009; Zhou *et al.*, 2010; Eom *et al.*, 2013b). In addition, novel technologies involving biodegradation and biotransformation (Ratlege, 1992), microfiltration (Scott *et al.*, 2001), and ultrafiltration (Belkacem *et al.*, 2007) have been developed for the treatment of oily wastewaters. Among the several separation technologies, microfiltration and ultrafiltration using membranes are the most promising methods to effectively meet the desired standards. The obvious advantages of membrane techniques in treating oily wastewater include their high oil-removal efficiency, low energy cost, low capital cost, and the absence of chemical additives (Cheryan and Rajagopalan, 1998; Abbasi *et al.*, 2010). Researchers have reported the effectiveness of microfiltration and ultrafiltration technologies for the treatment of oily wastewater using different membranes (Gorouhi *et al.*, 2006; Kroll *et al.*, 2010; Vasanth *et al.*, 2011a). Gorouhi *et al.* (2006) performed microfiltration of oily wastewater using a polypropylene membrane with a pore size of 0.2 μm. Microfiltration of oily wastewater was investigated (Scott *et al.*, 1994) using various polymeric membranes from materials such as polysulfone, nylon, and polytetrafluoroethylene, all of which possessed a mean pore size of 0.2 μm, and had reported oil-rejection rates of >90%.

Ceramic membranes are becoming increasingly important for the treatment of oily wastewater because their intrinsic nature offers many advantages over polymer

* E-mail address of corresponding author:
ywkim@uos.ac.kr
DOI: 10.1346/CCMN.2015.0630305

membranes, *e.g.* good chemical stability, stability at high temperature and pressure, high mechanical stability, longevity, good fouling stability, and catalytic properties (Bouzerara *et al.*, 2006; Emani *et al.*, 2013; Ha *et al.*, 2013b; Lee *et al*., 2014). Generally, ceramic membranes are prepared from alumina (Al_2O_3), zirconia (ZrO_2), titania (TiO_2), and silica (SiO_2). The application of ceramic membranes, however, is limited by the high cost of the base materials and by the sintering process at high temperatures. To overcome these drawbacks, attempts have been made to fabricate low-cost ceramic membranes using cost-effective raw materials (Table 1, Weir *et al.*, 2001; Shackelford and Lee, 2003; Khemakhem *et al.*, 2006; Saffaj *et al.*, 2006; Song *et al.*, 2006; Eom *et al*., 2014; Harabi *et al*., 2014; Belibi *et al*., 2015). Previous works have focused on the preparation of cost-effective membranes from natural raw materials and the characterization of physical and mechanical properties of those membranes. No systematic research has been done on the effect of pore size on the performance of low-cost ceramic membranes or on investigations of recycling for achieving further efficiency of the membranes fabricated from natural resources.

Several strategies have been suggested in the literature that may improve both the performance and cost-effectiveness of ceramic membranes: (1) modification of the composition of raw materials including more cost-effective raw materials such as diatomite and talc; (2) pore-size optimization of low-cost membranes by adjusting sintering temperature; and (3) recycling used membranes by a simple heat treatment. The objectives of the present study were to investigate: (1) the properties and filtration performance of low-cost ceramic membranes produced from a new composition satisfying point 1 listed above; (2) the effect of pore size on the properties of membranes produced from the composition satisfying point 2 above; and (3) the possibility of recycling the membranes by a simple burn-out process. Filtration experiments of synthetic oil-water emulsions were carried out to characterize the separation performance of the ceramic membranes prepared.

EXPERIMENTAL

Materials

Commercially available calcined diatomite (Celite 505, $Fe_2O_3 \leqslant 1.3\%$, $P_2O_5 \leqslant 0.1\%$, $TiO_2 \leqslant 0.2\%$, CaO $\leqslant 0.4\%$, MgO $\leqslant 0.4\%$, Celite Korea Co. Ltd., Seoul, Korea), kaolin (extra pure, Cl $\leqslant 0.04\%$, As $\leqslant 0.002\%$, Fe $\leqslant 0.05\%$, Pb $\leqslant 0.005\%$, Samchun Pure Chemical Co. Ltd., Pyeongtaek, Korea), bentonite (chemically pure, Yakuri Pure Chemicals Co. Ltd., Kyoto, Japan), talc (chemically pure, Samchun Pure Chemical Co. Ltd., Pyeongtaek, Korea), sodium borate (extra pure, Samchun Pure Chemical Co., Ltd., Pyeongtaek, Korea), and barium carbonate (reagent-grade, Daejung Chemicals and Metals Co. Ltd., Siheung, Korea) were used as the base materials. Diatomite and talc are low-cost non-clay silicate materials and kaolin and bentonite are low-cost clay materials. Sodium borate and barium carbonate were

Table 1. Raw materials and properties of low-cost ceramic membranes reported in the literature.

Author	Raw materials	Properties
Mohammadi *et al*. (2004)	kaolin	Pore size: 10 μm
Bouzerara *et al*. (2006)	kaolin and dolomite	Porosity: ~37−56% Pore size: ~0.02−7.68 μm Tensile strength: ~5−16 MPa
Vasanth *et al.* (2011a)	kaolin, quartz, and calcium carbonate	Porosity: ~20−30% Pore size: ~1.30−2.77 μm Flexural strength: ~34−46 MPa
Emani *et al.* (2013)	kaolin, quartz, calcium carbonate, sodium carbonate, boric acid, and sodium metasilicate	Porosity: ~35−39% Pore size: ~0.89−1.85 μm Fouling resistance: ~33.5−41.6%
Ha *et al.* (2013a)	diatomite, polymer spheres, starch, and carbon nanotube	Pore size: ~1−2 μm
Sahnoun and Baklouti (2013)	kaolin, phosphoric acid, and starch	Porosity: ~24−50% Rupture strength: ~2−19 MPa
Emani *et al*. (2014)	kaolin, quartz, calcium oxide, sodium oxide, boric acid, sodium metasilicate	Porosity: ~30−37% Pore size: ~2.33−3.23 μm Fouling resistance: ~15.5−29.5%
Harabi *et al*. (2014)	kaolin, calcite	Porosity: ~45−52% Pore size: ~1.8−17.6 μm Flexural strength: ~67−87 MPa
Belibi *et al*. (2015)	Cameroonian clay	Porosity: 42% Fouling resistance: ~62−66%

https://doi.org/10.1346/CCMN.2015.0630305 Published online by Cambridge University Press

added to increase the mechanical strength of membranes. A batch containing 48.6 wt.% diatomite, 18.8 wt.% kaolin, 14.8 wt.% bentonite, 14.8 wt.% talc, 2.0 wt.% sodium borate, and 1.0 wt.% barium carbonate was prepared by mixing the raw materials using Al_2O_3 grinding balls in distilled water. Polyethylene glycol was added as a binder. The milled slurry was dried and pressed uniaxially under an applied pressure of 50 MPa. The compacts were sintered at 1000, 1050, or 1100ºC for 1 h at a heating rate of 3ºC/min in air. The membranes sintered at 1000, 1050, or 1100ºC are designated as M1000, M1050, or M1100, respectively.

Characterization of properties

The bulk density of the ceramic membranes was calculated from the weight-to-volume ratio of samples. The apparent porosity of the ceramic membranes was measured using the Archimedes method. The open porosity and pore-size distribution were measured using mercury porosimetry (AutoPore IV 9500, Micromeritics, Norcross, Georgia, USA). X-ray diffraction (XRD, D8 Discover, Bruker AXS GmbH, Germany) was conducted on ground, randomly oriented powders using Ni-filtered CuKα radiation. The powdered samples were loaded into the well of a sample holder and pressed with a flat plate. The goniometer was three-axis. The operation voltage and current of the X-ray tube were 40 mV and 40 mA, respectively. The specific dimensions of the divergence and receiving slits were 0.1 and 0.2 mm, respectively. The anti-scatter slit was a Ni filter. Samples were scanned from 10 to 70º2θ, at a step size of 0.05º2θ and a counting time of 1 s/step.

Fracture surface morphology was examined using scanning electron microscopy (SEM, S4300, Hitachi Ltd., Hitachi, Japan). Carbon tape was used to mount samples on the copper substrate. The samples were coated using a Pt target in a vacuum of 2×10^{-8} torr. The SEM was operated at an accelerating voltage of 15 kV and a current of 15 mA in a vacuum of 1×10^{-7} torr. The imaging mode of the SEM was secondary electrons and the spot size was 30 μm. One (M1100) of the polished membranes with a Pt layer coating was analyzed by energy dispersive analysis (EDS, JSM-6010PLUS/LA, JEOL, Tokyo, Japan) at 20 kV and 30 mA in a vacuum of 1×10^{-5} torr. Elemental distributions of Na, B, and Ba were collected on the polished surface of the membrane for 1 h at 20 kV and 30 mA.

For flexural strength measurements, bar-shaped samples were cut to a size of 3 mm × 4 mm × 30 mm, and bending tests were performed at a constant cross-head speed of 0.5 mm/min using a three-point bending fixture with a span of 20 mm.

Filtration of pure water and oil-water emulsion

An oil-water emulsion with an oil concentration of 600 ppm was prepared by mixing kerosene (Daejung Chemicals and Metals Co. Ltd., Siheung, Korea) and distilled water with the surfactant polyoxyethylene sorbitan monooleate (Tween 80, Wako Pure Chemical Industries, Ltd., Osaka, Japan; 0.06 g/L) using an ultrasonic mixer for 1 h. The feed-oil concentration of 600 ppm is relatively large for the application of membrane technology. This high concentration was selected to test the performance of the present membranes under extreme conditions. The emulsion preparation was carried out at room temperature. The average droplet size in the stable oil-water emulsion was analyzed quantitatively by image analysis (Infinity Capture, Lumenera Co., Ottawa, Canada). The oil-water emulsion had an average droplet size of ~2.20 μm.

The home-made dead-end filtration setup used for the oil-water emulsion filtration tests (Figure 1) was constructed of stainless steel (capacity of ~11 L) and consisted of two parts, a cylindrical top part and a base plate with a provision to host the membrane. The membrane was placed on a perforated casing with a pair of O-rings and set in the bottom compartment. The upper compartment of the batch cell was pressurized by an air cylinder. The membrane was 4.6×10^{-2} m in diameter and 3.0×10^{-3} m thick, and the effective membrane area was 1.59×10^{-3} m^2.

The permeate flux (J_w) (m^3 m^{-2} h^{-1}) was calculated using the following equation:

$$J_w = Q/(A\ \Delta t) \quad (1)$$

where Q is the amount of permeate collected (m^3), A is the membrane area (m^2), and Δt is the sampling time (h).

Fouling resistance (FR) was calculated using the following equation (Emani *et al*., 2013):

$$FR\ (\%) = \{(J_{wi} - J_{wf})/J_{wi}\} \times 100 \quad (2)$$

where J_{wi} is the initial permeate flux and J_{wf} is the final permeate flux after fouling.

The oil filtration experiments were carried out with an oil-water emulsion using the ceramic membranes prepared with three different pore sizes (0.29 μm, 0.37 μm, and 0.67 μm) at an applied pressure of 303 kPa. After the first filtration, the low-cost ceramic membranes were heat-treated at 600ºC for 1 h at a heating rate of 3ºC/min in air to remove any organic contaminants introduced during the filtration process. After the heat-treatment, the second filtration experiment was carried out under the same conditions. All experiments were conducted at room temperature, and the oil-rejection rate (R) was calculated according to the following equation:

$$R\ (\%) = (1 - C_p/C_f) \times 100 \quad (3)$$

where C_p and C_f represent the oil concentrations in the permeate and feed, respectively. The oil concentrations in the feed and permeate were analyzed using a UV/VIS spectrophotometer (Evolution 60, Thermo Fisher Scientific Inc., Waltham, Massachusetts, USA) at an absorbance wavelength of 230 nm.

https://doi.org/10.1346/CCMN.2015.0630305 Published online by Cambridge University Press

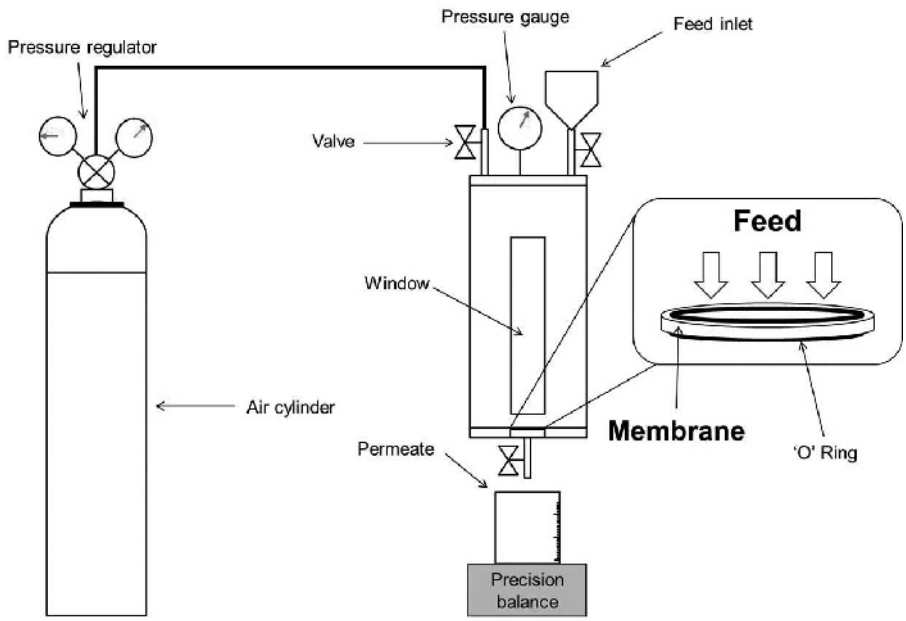

Figure 1. Experimental setup for filtration test.

RESULTS AND DISCUSSION

Membrane preparation and properties

Three different membranes were produced by partial sintering of raw materials. The membranes were prepared by the following procedure during heating and holding at 1000−1100ºC: (1) Expulsion of volatile species from the membrane body during heating. The volatile species include H_2O from bentonite, talc, and sodium borate, and CO_2 from barium carbonate. The escape of volatile species from the membrane body left pores in the membrane body. (2) The formation of a liquid phase by a reaction between sodium borate (melting point = 742ºC) and barium oxide (Lim *et al*., 2013). (3) The sodium borate-barium oxide-derived liquid formed a bonding phase between the non-clay silicate material-derived and clay material-derived grains and led to partial densification of the membrane body.

Analysis by XRD was carried out to identify the phases present in the M1000, M1050, and M1100 membranes (Figure 2). The M1000 membrane consisted of β-cristobalite, α-quartz, enstatite, and albite. The intensity of α-quartz peaks decreased with increasing sintering temperature, whereas the intensity of β-cristobalite peaks increased with increasing sintering temperature, indicating that the transition of α-quartz to β-cristobalite occurred at high sintering temperature. The M1100 membrane consisted of β-cristobalite, enstatite, albite, and α-quartz. β-cristobalite and α-quartz are derived from diatomite, enstatite is derived from talc, and albite is derived from bentonite and kaolin. Sodium borate and barium oxide or any of their compounds were not detected because of the small amount added (2 wt.% sodium borate and 1 wt.% barium carbonate).

The microstructures of the low-cost ceramic membranes (Figure 3) consisted of non-clay silicate material-derived and clay material-derived grains, as well as the sodium borate-barium oxide-derived bonding phase. A liquid phase was formed from sodium borate-barium oxide additives during sintering, and the liquid phase acted as an adhesive to bind the non-clay silicate material-derived and clay material-derived grains (Lim *et al.*, 2013). The grains were well bonded to each other by a binder phase (Figures 3 and 4). Dot mapping of B, Na, and Ba by EDS (Figure 4) revealed qualitatively that those elements are distributed on the surface of crystalline grains (β-cristobalite, α-quartz, enstatite, and albite). The B- and Na-depleted regions are the polished surfaces of crystalline grains, *i.e.* the center of the grains. In contrast, Ba was distributed more homogeneously throughout the specimen (M1100), compared to B and Na. The EDS results suggest that the sodium borate-barium oxide-derived liquid phase was mostly distributed on the surface of the non-clay silicate material-derived and clay material-derived grains and acted as a binder between those grains. A partial penetration of Ba into the non-clay silicate material-derived and clay material-derived grains occurred by a diffusional process during sintering, and the enhanced diffusion of Ba compared to that of B and Na might be attributed to the affinity of Ba with non-clay silicate materials.

The M1000 and M1050 membranes partially maintained the unique pore structure of the fossilized skeleton of diatoms (diatomite) when sintered at 1000 and 1050ºC (arrows in Figure 3a,c), whereas the M1100

https://doi.org/10.1346/CCMN.2015.0630305 Published online by Cambridge University Press

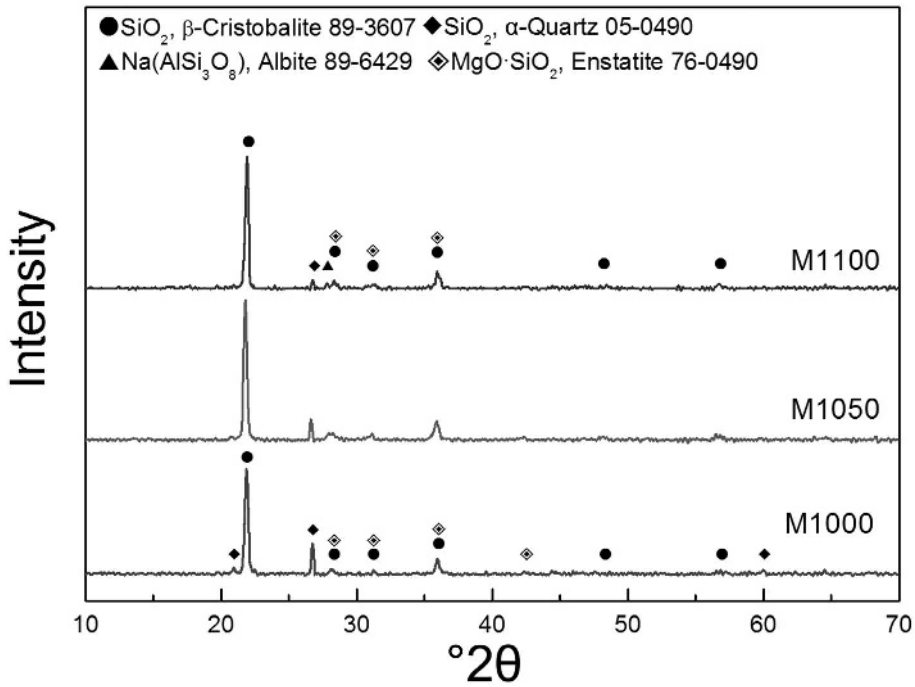

Figure 2. XRD patterns of the low-cost ceramic membranes. M1000, M1050, and M1100 denote membranes sintered at 1000ºC, 1050ºC, and 1100ºC, respectively. The numbers after the mineral names in the figure denote file numbers of the Joint Committee on Powder Diffraction Standards (JCPDS).

membrane consisted of a dense structure with a well developed grain structure (Figures 3e) due to the densification and coalescence of diatoms when sintered at 1100ºC. Sintering temperature influenced the pore structure of the membranes. The pore morphology changed from irregular to spherical as the sintering temperature increased. Moreover, the pore size increased with increasing sintering temperature. The pore morphology of the membrane surface was irregular in the M1000 and M1050 membranes, whereas in the M1100 membranes it was mostly equidimensional (Figure 3b,d,f). The irregularly shaped pores were derived from the inter-particle spaces in the green compacts, whereas the equidimensional pores originated from the coalescence of diatoms. The interconnected pore channels of the low-cost ceramic membranes were clearly observed at greater magnification (Figure 5). The pore-size distributions of the M1000, M1050, and M1100 membranes showed a unimodal distribution (Figure 6). The average pore diameter and open porosity increased from 0.29 μm to 0.67 μm and 32.2% to 34.1%, respectively, as the sintering temperature increased from 1000ºC to 1100ºC (Figure 6, Table 2). This type of pore growth with increasing sintering temperature has been observed many times in other porous ceramics (Eom *et al.*, 2008; Kim *et al.*, 2008; Manoj Kumar and Kim, 2010; Vasanth *et al.*, 2011b; Eom *et al.*, 2013a). The pore growth was attributed to pore coalescence during the sintering process. The average pore sizes of the membranes in the present study (0.29–0.67 μm) corresponded to a suitable pore-size range for microfiltration.

The bulk densities of the ceramic membranes (Table 2) were 1.55–1.57 g/cm^3 when sintered at 1000–1100ºC. The total porosity and open porosity of the ceramic membranes (Table 2) increased from 34.6% to 36.3% and from 32.2% to 34.1%, respectively, with increasing sintering temperature. These results are

Table 2. Density, porosity, and flexural strength of the low-cost ceramic membranes.

Sample designation	Sintering temperature (ºC)	Density (g/cm^3)	Total porosity (%)	Open porosity (%)	Flexural strength (MPa)
M1000	1000	1.57 ± 0.03	34.6 ± 1.2	32.2	32.2 ± 2.9
M1050	1050	1.56 ± 0.05	35.6 ± 2.3	33.0	30.1 ± 5.5
M1100	1100	1.55 ± 0.04	36.3 ± 1.6	34.1	27.9 ± 4.7

https://doi.org/10.1346/CCMN.2015.0630305 Published online by Cambridge University Press

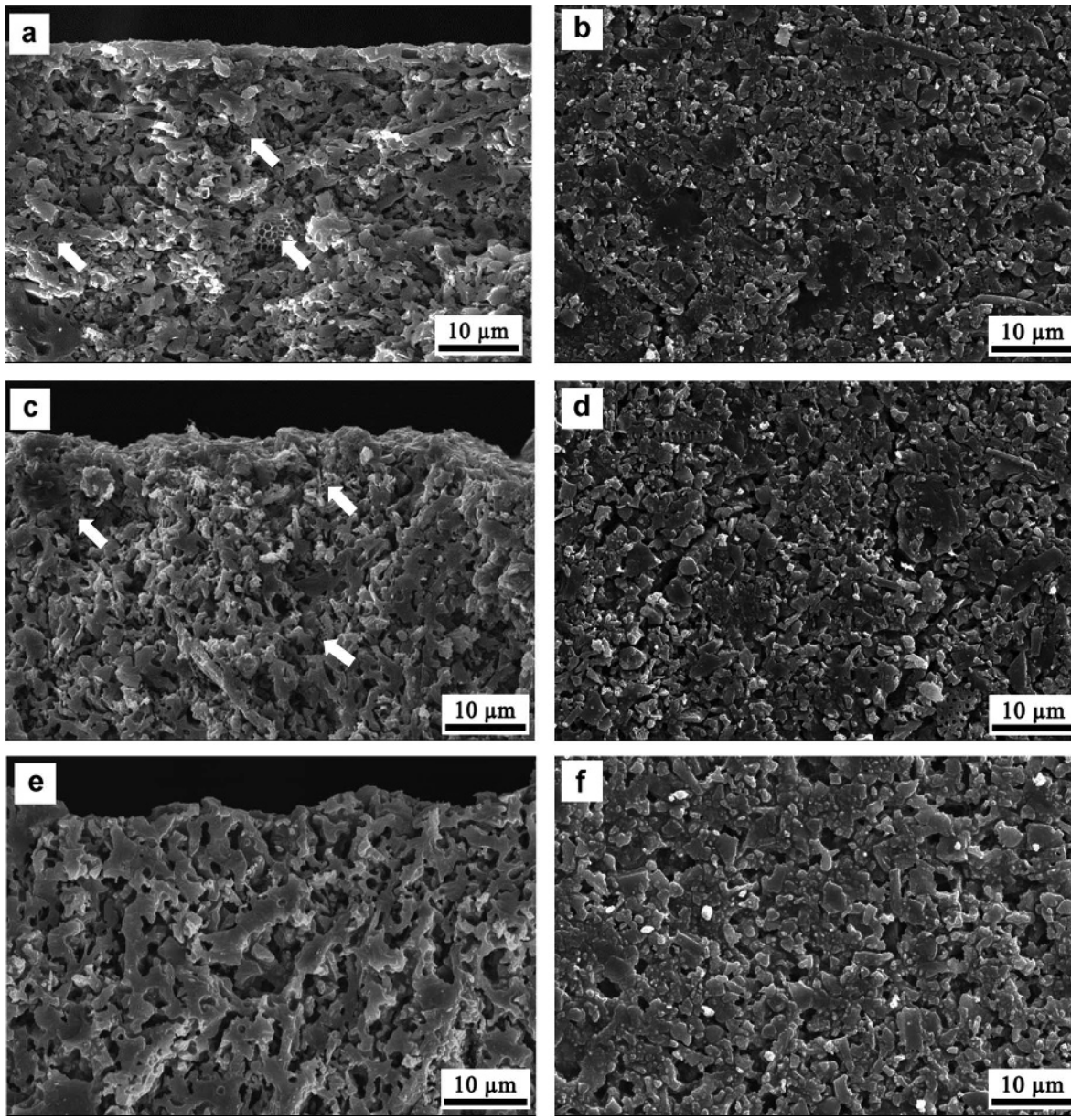

Figure 3. SEM images of the low-cost ceramic membranes sintered at various temperatures: (a) cross-section of M1000; (b) surface of M1000; (c) cross-section of M1050; (d) surface of M1050; (e) cross-section of M1100; and (f) surface of M1100 membranes. Arrows indicate the fossilized skeletons of diatoms.

consistent with the SEM images (Figure 3). The increase in porosity with increasing temperature is due to the greater possibility of pore interconnection as a result of pore coalescence during sintering at higher temperatures. This suggests that adjusting the sintering temperature is an efficient way of controlling the porosity as well as pore size.

The flexural strength of the ceramic membranes (Table 2) decreased from ~32 MPa to ~28 MPa as the sintering temperature increased from 1000ºC to 1100ºC. The decrease in strength with increasing sintering temperature was attributed to the increased total porosity from 34.6% to 36.3% and the increased pore size from 0.29 μm to 0.67 μm. In general, flexural strength tends to decrease with increasing porosity and increasing pore size (Eom and Kim, 2008; Lim *et al.*, 2013). This tendency has also been observed in many other porous ceramics and is attributed to the greater probability of pore coalescence at the larger porosity under load (Eom *et al.*, 2013a). The typical flexural strengths of the M1000, M1050, and M1100 membranes were 32.2 MPa with a porosity of 34.6%, 30.1 MPa with a porosity of

https://doi.org/10.1346/CCMN.2015.0630305 Published online by Cambridge University Press

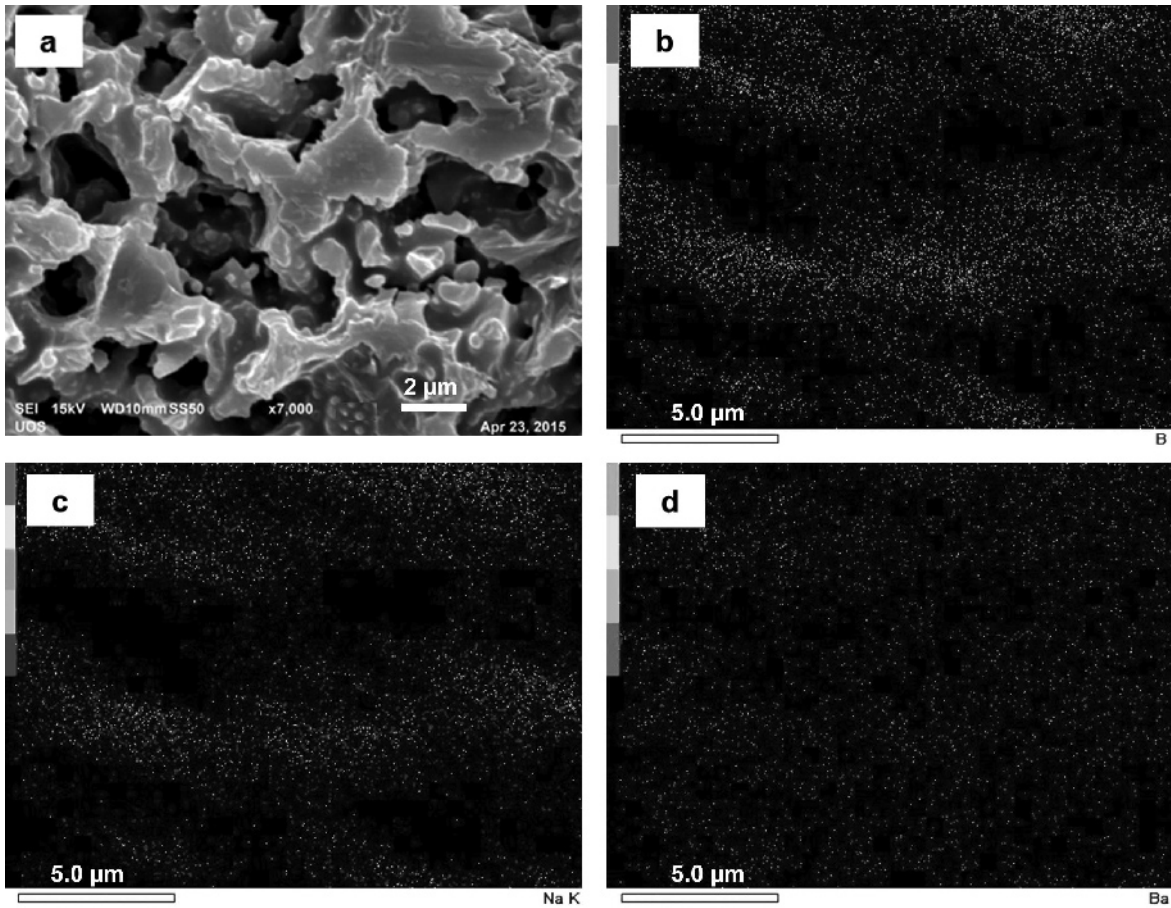

Figure 4. SEM image and qualitative compositional maps of the M1100 membrane: (a) SEM image; (b) boron; (c) sodium; and (d) barium elemental distribution.

35.6%, and 27.9 MPa with a porosity of 36.3%, respectively. Flexural strengths of 11 MPa with a porosity of 35% and 28 MPa with a porosity of 30% have been reported in clay-based membranes fabricated using kaolin, quartz, calcium carbonate, sodium carbonate, boric acid, and sodium metasilicate (Vasanth *et al.*, 2011b). Flexural strengths of ~12 MPa with a porosity of ~35% for a membrane prepared using Moroccan clay (Saffaj *et al.*, 2006), 34 MPa with a porosity of 30% for membranes prepared from kaolin, quartz, calcium carbonate, and titanium dioxide (Vasanth *et al.*, 2013), and 19 MPa with a porosity of 37% for the membranes prepared from kaolin and sodium borate (Eom *et al.*, 2013b) have been reported for clay-based membranes. Thus, the flexural strengths of the present membranes are superior or at least equivalent to the reported values, indicating the beneficial effect of sodium borate and barium carbonate additives in strengthening the diatomite-, kaolin-, bentonite-, and talc-based membranes. The flexural strength values of the membranes obtained in the present study are sufficient for use in industrial applications of the membranes for oily wastewater treatment.

Microfiltration of an oil-water emulsion

The permeate flux of each membrane at 303 kPa with an initial oil concentration of 600 mg/L decreased rapidly within 60 min and then decreased gradually to achieve a steady-state value after 100 min (Figure 7). The rapid flux decrease during the early stage of filtration can be explained by the pore-blocking phenomenon in the early stage of permeation. The formation of a cake layer on the membrane surface led to partial pore closure in the membranes, resulting in a decrease in the permeate flux (Salahi *et al.*, 2010b; Abbasi *et al.*, 2010; Eom *et al.*, 2014). As the filtration time increased, the pore-blocking process gradually became insignificant and the flux reached a steady-state value. Among the membranes, the smallest flux-decline rate was observed for the M1000 membrane, and the largest flux-decline rate was observed for the M1100 membrane. For the three membranes, the fouling resistance was in the order: M1100 (78.2%) > M1050 (65.2%) > M1000 (63.5%), indicating that the fouling resistance is greater when the pore size is larger. These results are consistent with those obtained by Eom *et al.* (2014) using a ceramic membrane fabricated with a

https://doi.org/10.1346/CCMN.2015.0630305 Published online by Cambridge University Press

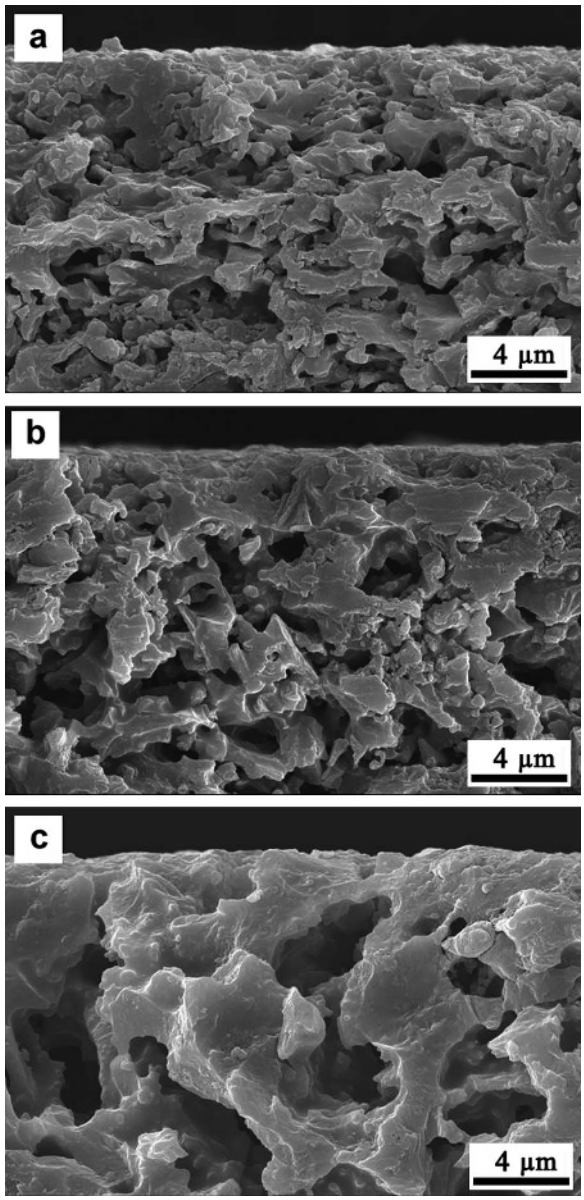

Figure 5. Pore structures of the low-cost ceramic membranes sintered at various temperatures: (a) cross-section of M1000; (b) cross-section of M1050; and (c) cross-section of M1100 membranes.

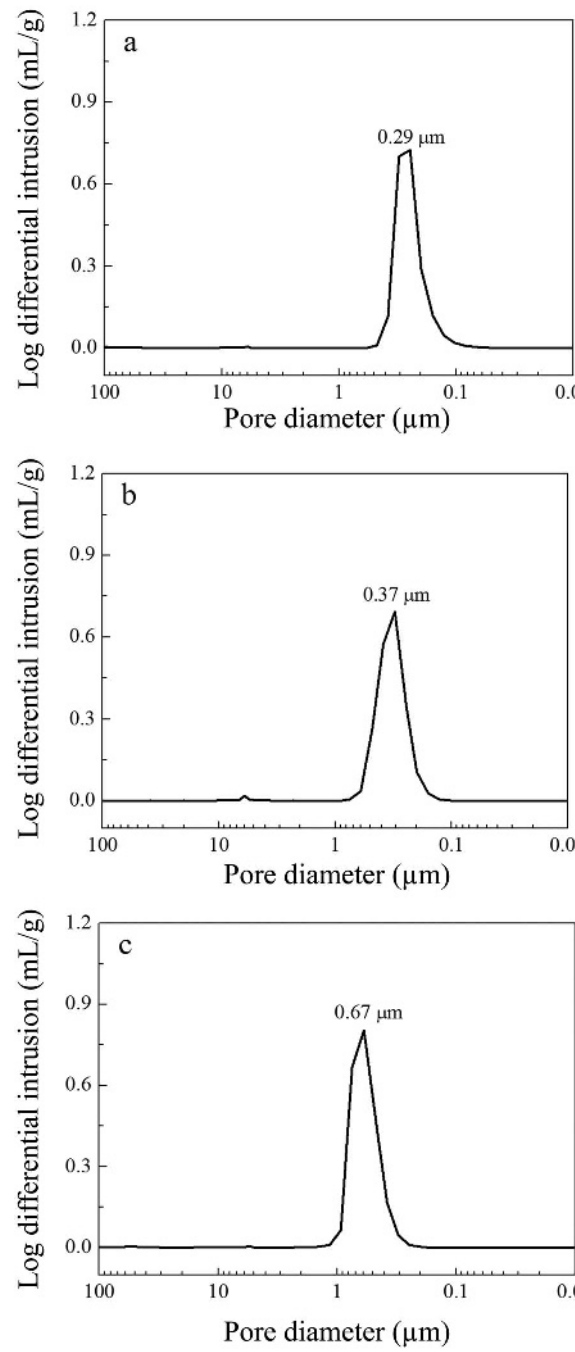

Figure 6. Pore-size distribution of the low-cost ceramic membranes: (a) M1000; (b) M1050; and (c) M1100 membranes.

mixture of kaolin, bentonite, and talc and from a ceramic membrane fabricated by Vasanth *et al*. (2013) using a mixture of kaolin, quartz, calcium carbonate, and TiO_2. The steady-state fluxes of M1000 and M1100 after 120 min of filtration were 2.5×10^{-5} $m^3m^{-2}s^{-1}$ and 2.8×10^{-5} $m^3m^{-2}s^{-1}$, respectively.

After the oily water filtration at 303 kPa for 120 min, the pores on and beneath the M1050 membrane surface were filled with the rejected oil cake in the oil-water emulsion (Figure 8). The SSAs of the virgin M1000, M1050, and M1100 membranes were 1.72, 1.53, and 0.92 m^2/g, respectively (Table 3). With increasing sintering temperature, the SSA of the membranes decreased due to pore coalescence, leading to an increase in pore size. After 120 min of filtration with a feed-oil concentration of 600 mg/L at a pressure of 303 kPa, the specific surface areas of the M1000, M1050, and M1100 membranes decreased to 1.56 m^2/g, 1.25 m^2/g, and 0.84 m^2/g, respectively. The

https://doi.org/10.1346/CCMN.2015.0630305 Published online by Cambridge University Press

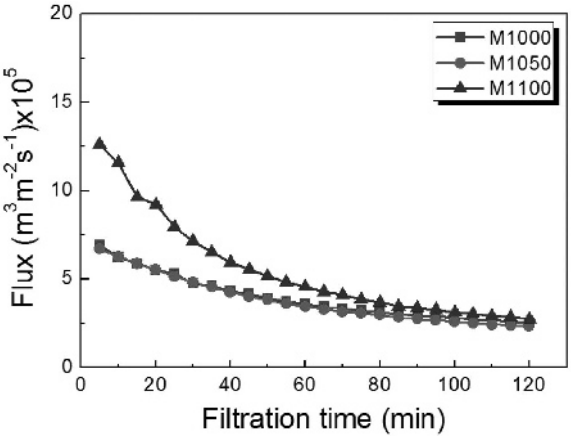

Figure 7. Variation of flux with time for the first filtration of a feed with an initial oil concentration of 600 mg/L at an applied pressure of 303 kPa.

surface areas of the membranes decreased by 8.7−18.3% after the filtration. The oil-rejection rates of the M1000, M1050, and M1100 membranes at 303 kPa were 84.1%, 84.2%, and 86.1%, respectively (Table 4).

Recycling the ceramic membranes

To investigate the possibility of recycling the membrane, after use, the membranes were heat treated at 600ºC for 1 h in air. By comparing the images in the M1050 membrane after 120 min of filtration (Figure 8) and the burned-out M1050 membrane (Figure 9), most of the pores on the membrane surface and inside the pores near the surface are noted to have been recovered and opened by burning out of the oil cake during heat treatment. After the heat treatment, the specific surface areas of the M1000, M1050, and M1100 membranes increased to 1.73 m^2 g^{-1}, 1.46 m^2 g^{-1}, and 0.88 m^2 g^{-1}, respectively. These values correspond to 100%, 95.4%, and 95.7% of the SSAs of the virgin M1000, M1050, and M1100 membranes; in other words, >95% of the SSAs of the virgin membranes were recovered in all membranes

Table 3. SSA of the low-cost ceramic membranes.

Sample designation	— Specific surface area (m^2/g) – As sintered	After filtration	After burn-out
M1000	1.72	1.56	1.73
M1050	1.53	1.25	1.46
M1100	0.92	0.84	0.88

by simple heat treatment at 600ºC for 1 h in air. The increase in specific surface area denotes the increase in total permeable area in the membranes.

The variation in permeate flux (oil-water emulsion) of the ceramic membranes used (second time filtration) and the burned-out ceramic membranes (referred to hereafter as recycled membranes) as a function of time at 303 kPa with an initial oil concentration of 600 mg/L showed that the permeate flux of all of the membranes used, as well as that of the recycled M1000 and M1050 membranes, decreased slowly within 60 min and achieved a near steady-state value after 80 min of filtration (Figure 10). In contrast, the recycled M1100 membranes showed very similar behavior to the virgin M1100 membranes, *i.e.* an initial rapid decline after 60 min of filtration, followed by a gradual decrease before eventually achieving a steady-state value after 100 min of filtration.

The slower decrease in flux of the used membranes compared to the virgin membranes was due to the fact that the pore-blocking process became progressively insignificant as the filtration proceeded and the flux reached steady state. The recycled M1000 and M1050 membranes showed significantly less fouling resistance than the equivalent virgin membranes. The fouling resistances of the virgin M1000 and M1050 membranes were 63.5% and 65.2%, respectively, whereas the fouling resistances of the recycled M1000 and M1050 membranes were 27.1% and 30.0%, respectively. Furthermore, the steady-state values of the fluxes of

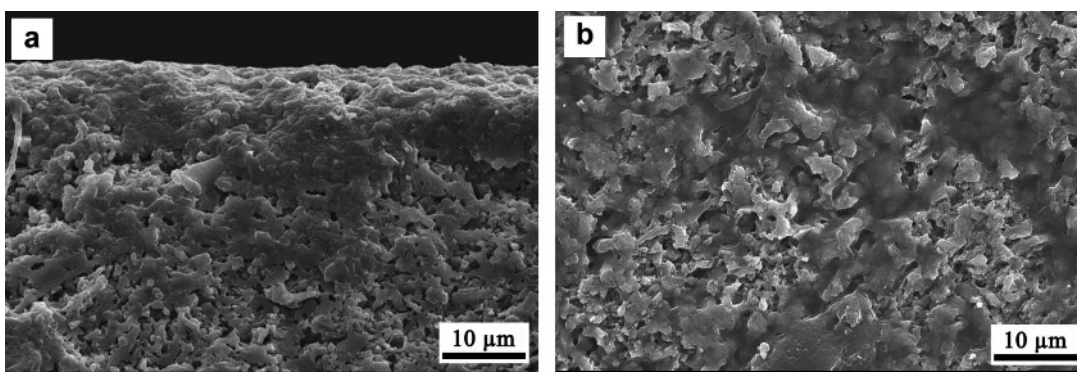

Figure 8. SEM images of the low-cost ceramic membrane (M1050) sintered at 1050ºC after 120 min of oily water filtration at 303 kPa: (a) cross-section of the M1050; and (b) surface of the M1050 membrane.

https://doi.org/10.1346/CCMN.2015.0630305 Published online by Cambridge University Press

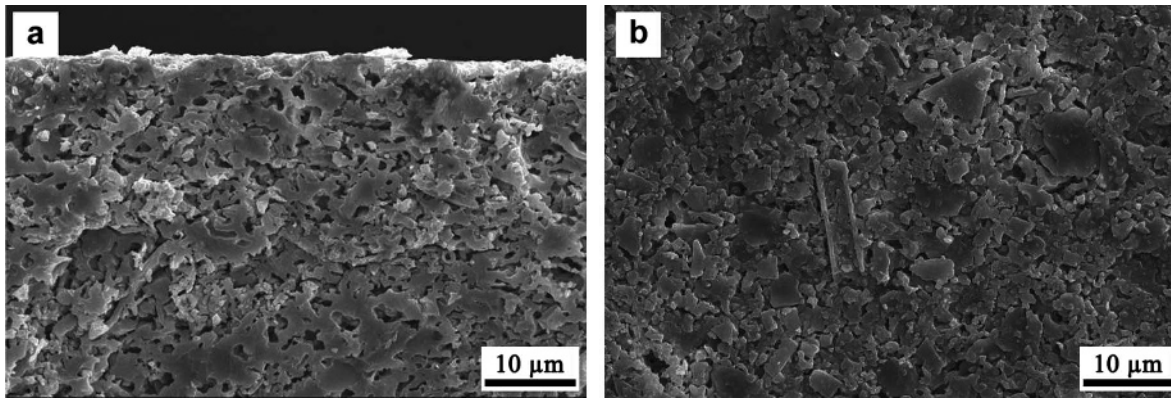

Figure 9. SEM micrographs of low-cost ceramic membranes sintered at 1050ºC and subsequently heat treated at 600ºC for 1 h in air after the first filtration: (a) cross-section of M1050 and (b) surface of M1050 membrane.

the recycled M1000 and M1050 membranes were 5.4×10^{-5} $m^3m^{-2}s^{-1}$ and 5.0×10^{-5} $m^3m^{-2}s^{-1}$, respectively, which are more than double the flux values of the virgin membranes (2.5×10^{-5} $m^3m^{-2}s^{-1}$ for M1000 and 2.3×10^{-5} $m^3m^{-2}s^{-1}$ for M1050). These results suggest that the burn-out process removes the oil cake, recovers the SSA of the membranes to a value close to that of virgin membranes in order to produce a more permeable membrane area, and changes slightly the pore structure due to partial sintering, resulting in reduced fouling.

The recycled M1100 membrane showed quite different flux behavior compared to that of the recycled M1000 and M1050 membranes (Figure 10). The fouling resistance values of the virgin and recycled M1100 membranes were 78.2% and 72.0%, respectively. The greater fouling resistance value of the M1100 membranes was due to the larger pore size of the membranes compared to those of the other membranes, which leads to a greater fouling resistance (Vasanth *et al*. 2013; Eom *et al*., 2014). These results suggest that the pore size of the M1100 membrane (0.67 μm) is too large to produce a smaller fouling rate, and the preferred pore size of the membranes for oily wastewater filtration should be <0.4 μm. The pore size of 0.4 μm is also a requirement for bio-filters to remove bacterial cells the sizes of which are typically 0.5–5.0 μm long.

The fouling resistance decreased slightly from 63.5–78.2% for the virgin membranes to 52.7–73.1% for the used membranes. After the second filtration, the steady-state values of flux decreased from 2.3×10^{-5} – 2.8×10^{-5} $m^3m^{-2}s^{-1}$ for the virgin membranes to 1.7×10^{-5} – 2.4×10^{-5} $m^3m^{-2}s^{-1}$ for the used membranes, indicating that fouling proceeds slowly with increasing filtration time.

The oil-rejection rates for the used membranes (Table 4) were slightly greater (87.8–88.3%) than those of the virgin membranes (84.1–86.1%). The increase in oil rejection rate, however, accompanied loss of flux (Figures 7, 10). The increase in rejection rate after the second filtration was due to the decreased pore size after the first filtration due to pore blockage by the oil cake. The decreased pore size caused by the formation of a cake layer on the membrane surface led to lower permeate flux, while the rejection rate of the membranes increased. In contrast, the oil-rejection rates for the recycled membranes increased significantly (88.0–92.9%) compared to those of virgin membranes (84.1–86.1%). Furthermore, the increase in oil-rejection rate accompanied the increase in flux (Figure 10). The

Table 4. Oil-rejection rate of the low-cost ceramic membranes for a feed-oil concentration of 600 mg/L at an applied pressure of 303 kPa.

Sample designation	1st filtration	– 2nd filtration –	
		No burn-out (Used)	Burn-out (Recycled)
M1000	84.1	87.8	92.9
M1050	84.2	88.3	90.4
M1100	86.1	88.0	88.0

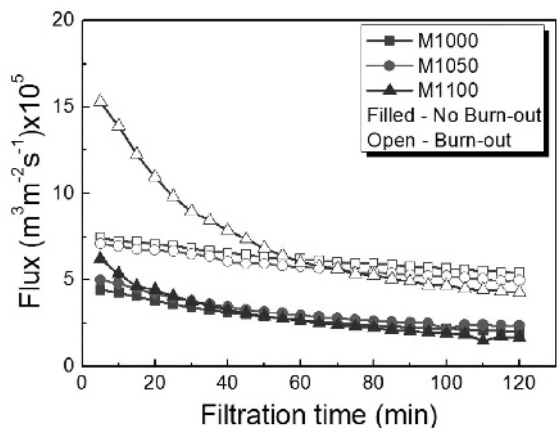

Figure 10. Variation of flux with time for the second filtration of a feed with an initial oil concentration of 600 mg/L at an applied pressure of 303 kPa.

https://doi.org/10.1346/CCMN.2015.0630305 Published online by Cambridge University Press

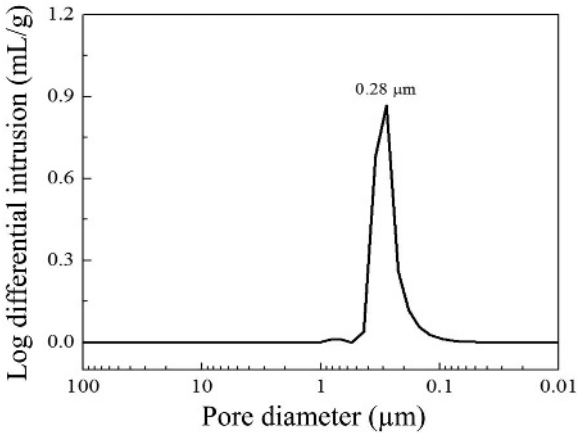

Figure 11. Pore-size distribution of the recycled M1000 membrane, which was sintered at 1000ºC and subsequently heat-treated at 600ºC for 1 h in air after the first filtration.

maximum rejection rate (92.9%) was obtained with the recycled M1000 membrane; this because it has the smallest pore size of all of the membranes. The pore-size distribution of the recycled M1000 membrane (Figure 11) showed a unimodal distribution with an average pore size of 0.28 μm. The pore size was slightly smaller than that of virgin M1000 membrane (0.29 μm, Figure 6a). The decrease was caused by a partial sintering of the membrane body during the burn-out process. The decrease in the average pore size of the recycled M1000 membrane increased the oil-rejection rate (Table 4) and decreased fouling resistance, resulting in increased flux (Figure 10).

Comparisons of oil-rejection rates of low-cost ceramic membranes reported in the literature (Table 5) showed that the oil-rejection rates of the membranes studied here, especially those of the recycled membranes (88.0–92.9%), are comparable with the literature values or better, except for the rejection rate (97.9%) reported by Emani *et al*. (2014), a value which was obtained when crude oil was used as a feed. The molecular weight of crude oil is much greater than that of kerosene. As larger molecules with greater molecular weights are rejected more efficiently than smaller molecules, the high rejection rate obtained by Emani *et al*. (2014) was understandable.

In summary, the burn-out process for used membranes at 600ºC resulted in the following changes: (1) >95% of the specific surface area of the virgin membranes was recovered; (2) the fouling rate decreased from 63.5–78.2% to 27.1–73.1%; (3) the steady-state flux increased from 2.3×10^{-5}–2.8×10^{-5} $m^3m^{-2}s^{-1}$ to 4.3×10^{-5}–5.4×10^{-5} $m^3m^{-2}s^{-1}$; (4) the oil-rejection rate increased from 84.1–86.1% to 88.0–92.9%. The present results suggest that the low-cost ceramic membranes used for oily wastewater filtration can be recycled by simple heat-treatment at 600ºC in air. The present results also suggest that further improvement in the oil rejection rate and flux are possible by optimizing the pore size of the membranes and by means of the burn-out process.

One approach for tailoring the properties of membranes is to modify their surface. Further improvement in oil-rejection rate might be achieved by applying top-layer coatings on the silicate and clay mineral-based membranes with a minimal increase in cost. For example, the introduction of an alumina (Al_2O_3) coating layer on the silicate- and clay mineral-based membranes provides an enhanced hydrophilic character to the membrane surface (Li *et al.*, 2009). The hydrophilic surface prevents oil droplets from adhering to the membrane surface, thus weakening membrane fouling and, probably, increasing the oil-rejection rate.

CONCLUSIONS

Low-cost ceramic membranes with a pore size of 0.29–0.67 μm were prepared successfully by a simple pressing route using low-cost base materials including diatomite, kaolin, bentonite, talc, sodium borate, and barium carbonate. The porosity and average pore size of

Table 5. Oil-rejection rate of various membranes reported in the literature.

Author	Membrane composition	Condition	Rejection rate (%)
Abbasi *et al.* (2010)	Mullite	Oil concentration: 250 mg/L Applied pressure: 300 kPa	85.4
Salahi *et al*. (2010a)	Polysulfone	Oil concentration: 80 mg/L Applied pressure: 300 kPa	66.3
Abadi *et al.* (2011)	Alumina	Oil concentration: 30 mg/L Applied pressure: 100 kPa	85
Vasanth *et al.* (2011a)	Clay	Oil concentration: 250 mg/L Applied pressure: 69 kPa	85
Emani *et al*. (2014)	Kaolin, quartz, calcium oxide, sodium oxide	Crude oil concentration: 400 mg/L Applied pressure: 207 kPa	97.9
Pagidi *et al*. (2014)	Polysulfone	Oil concentration: 2000 mg/L Applied pressure: 410 kPa	83.3

https://doi.org/10.1346/CCMN.2015.0630305 Published online by Cambridge University Press

the membranes increased from 34.6% to 36.3% and from 0.29 μm to 0.67 μm, respectively, as the sintering temperature was increased from 1000ºC to 1100ºC. The membranes prepared exhibited good flexural strength in the range of 28–32 MPa, depending on the porosity of the membranes. The membranes prepared had oil-rejection rates of 84.1–86.1% with a feed concentration of 600 mg/L and a steady-state flux of 2.3×10^{-5}–2.8×10^{-5} $m^3m^{-2}s^{-1}$ at an applied pressure of 303 kPa. As the fouling resistance of the low-cost ceramic membranes decreased with decrease in pore size, the preferred pore size of the membranes for oily-wastewater filtration should be <0.4 μm.

A simple burn-out process of the used membranes at 600ºC in air recovered >95% of the SSA of the virgin membranes, decreased the fouling rate from 63.5–78.2% to 27.1–73.1%, increased the steady-state flux from 2.3×10^{-5}–2.8×10^{-5} $m^3m^{-2}s^{-1}$ to 4.3×10^{-5}–5.4×10^{-5} $m^3m^{-2}s^{-1}$, and increased the oil-rejection rate from 84.1–86.1% to 88.0–92.9%. The present results suggest that the low-cost ceramic membranes used for oily-wastewater filtration can be recycled by simple heat treatment at 600ºC in air.

ACKNOWLEDGMENTS

The present study was supported financially by the Fundamental Research Program of the Korea Institute of Materials Science (KIMS).

REFERENCES

Abadi, S.R.H., Sebzari, M.R., Hemati, M., Rekabdar, F., and Mohammadi, T. (2011) Ceramic membrane performance in microfiltration of oily wastewater. *Desalination*, **265**, 222–228.

Abbasi, M., Mirfendereski, M., Nikbakht, M., Golshenas, M., and Mohammadi, T. (2010) Performance study of mullite and mullite–alumina ceramic MF membranes for oily wastewaters treatment. *Desalination*, **259**, 169–178.

Belibi, P.B., Nguemtchouin, M.M.G., Rivallin, M., Nsami, J.N., Sieliechi, J., Cerneaux, S., Ngassoum, M.B., and Cretin, M. (2015) Microfiltration ceramic membranes from local Cameroonian clay applicable to water treatment. *Ceramics International*, **41**, 2752–2759.

Belkacem, M., Bahlouli, M., Mraoui, A., and Bensadok, K. (2007) Treatment of oil-water emulsion by ultrafiltration: a numerical approach. *Desalination*, **206**, 433–439.

Bouzerara, F., Harabi, A., Achour, S., and Larbot, A. (2006) Porous ceramic supports for membranes prepared from kaolin and doloma mixtures. *Journal of the European Ceramic Society*, **26**, 1663–1671.

Chen, W., Peng, J., Su, Y., Zheng, L., Wang, L., and Jiang, Z. (2009) Separation of oil/water emulsion using Pluronic F127 modified polyethersulfone ultrafiltration membranes. *Separation and Purification Technology*, **66**, 591–597.

Cheryan, M. and Rajagopalan, N. (1998) Membrane processing of oily streams. Wastewater treatment and waste reduction. *Journal of Membrane Science*, **151**, 13–28.

Emani, S., Uppaluri, R., and Purkait, M.K. (2013) Preparation and characterization of low cost ceramic membranes for mosambi juice clarification. *Desalination*, **317**, 32–40.

Emani, S., Uppaluri, R., and Purkait, M.K. (2014) Microfiltration of oil-water emulsions using low cost ceramic membranes prepared with the uniaxial dry compaction method. *Ceramics International*, **40**, 1155–1164.

Eom, J.H. and Kim, Y.W. (2008) Effect of template size on microstructure and strength of porous silicon carbide ceramics. *Journal of the Ceramic Society of Japan*, **116**, 1159–1163.

Eom, J.H., Kim, Y.W., Song, I.H., and Kim, H.D. (2008) Processing and properties of polysiloxane-derived porous silicon carbide ceramics using hollow microspheres as templates. *Journal of the European Ceramic Society*, **28**, 1029–1035.

Eom, J.H., Kim, Y.W., and Raju, S. (2013a) Processing and properties of macroporous silicon carbide ceramics: A review. *Journal of Asian Ceramic Societies*, **1**, 220–242.

Eom, J.H., Kim, Y.W., and Song, I.H. (2013b) Processing of kaolin-based microfiltration membranes. *Journal of the Korean Ceramic Society*, **50**, 341–347.

Eom, J.-H., Kim, Y.-W., Yun, S.-H., and Song, I.-H. (2014) Low-cost clay-based membranes for oily wastewater treatment. *Journal of the Ceramic Society of Japan*, **122**, 788–794.

Ezzati, A., Gorouhi, E., and Mohammadi, T. (2005) Separation of water in oil emulsions using microfiltration. *Desalination*, **185**, 371–382.

Gorouhi, E., Sadrzadeh, M., and Mohammadi, T. (2006) Microfiltration of oily wastewater using PP hydrophobic membrane. *Desalination*, **200**, 319–321.

Ha, J., Oh, E., and Song, I. (2013a) The effect of sacrificial templates on the pore characteristics of sintered diatomite membranes. *Journal of the Ceramic Society of Japan*, **121**, 940–945.

Ha, J.-H., Oh, E., Ahmad, R., and Song, I.-H. (2013b) The effects of pore structures on the air permeation properties of sintered diatomite. *Ceramics International*, **39**, 3881–3884.

Hajasgarkhani, M.A., Mousavi, S.M., and Saljoughi, E. (2013) Effects of coagulation-bath temperature and montmorillonite nanoclay content on asymmetric cellulose acetate butyrate membranes. *Clays and Clay Minerals*, **61**, 541–550.

Harabi, A., Zenikheri, F., Boudaira, B., Bouzerara, F., Guechi, A., and Foughali, L. (2014) A new and economic approach to fabricate resistant porous membrane supports using kaolin and $CaCO_3$. *Journal of the European Ceramic Society*, **34**, 1329–1340.

Khemakhem, S., Larbot, A., and Ben Amar, R. (2006) Study of performances of ceramic microfiltration membrane from Tunisian clay applied to cuttlefish effluents treatment. *Desalination*, **200**, 307–309.

Kim, Y.W., Eom, J.H., Wang, C., and Park, C.B. (2008) Processing of porous silicon carbide ceramics from carbon-filled polysiloxane by extrusion and carbothermal reduction. *Journal of the American Ceramic Society*, **91**, 1361–1364.

Kroll, S., Treccani, L., Rezwan, K., and Grathwohl, G. (2010) Development and characterisation of functionalised ceramic microtubes for bacteria filtration. *Journal of Membrane Science*, **365**, 447–455.

Kumara, S.M. and Roy, S. (2008) Filtration characteristics in dead-end microfiltration of living *Saccharomyces cerevisiae* cells by alumina membranes. *Desalination*, **229**, 348–361.

Lee, Y.I., Eom, J.H., Kim, Y.W., and Song, I.H. (2014) Effect of clay-mineral composition on flexural strength of clay-based membranes. *Journal of the Korean Ceramic Society*, **51**, 380–385.

Li, L., Ding, L., Tu, Z., Wan, Y., Clausse, D., and Lanoiselle, J.L. (2009) Recovery of linseed oil dispersed within an oil-in-water emulsion using hydrophilic membrane by rotating disk filtration system. *Journal of Membrane Science*, **342**, 70–79.

Lim, K.Y., Kim, Y.W., and Song, I.H. (2013) Porous sodium

borate-bonded SiC ceramics. *Ceramics International*, **39**, 6827–6834.

Manoj Kumar, B.V. and Kim, Y.W. (2010) Processing of polysiloxane-derived porous ceramics: a review. *Science and Technology of Advanced Materials*, **11**, 044303.

Mohammadi, T., Pak, A., Karbassian, M., and Golshan, M. (2004) Effect of operating conditions on microfiltration of an oil-water emulsion by a kaolin membrane. *Desalination*, **168**, 201–205.

Mueller, J., Cen, Y., and Davis, R.H. (1997) Crossflow microfiltration of oily water. *Journal of Membrane Science*, **129**, 221–235.

Pagidi, A., Saranya, R., Arthanareeswaran, G., Ismail, F., and Matsuura, T. (2014) Enhanced oil–water separation using polysulfone membranes modified with polymeric additives. *Desalination*, **344**, 280–288.

Ratlege, C. (1992) Mini review compilation. Biodegradation and biotransformations of oils and fats – introduction. *Journal of Chemical Technology and Biotechnology*, **55**, 397–398.

Saffaj, N., Persin, M., Younsi, S.A., Albizane, A., Cretin, M., and Larbot, A. (2006) Elaboration and characterization of microfiltration and ultrafiltration membranes deposited on raw support prepared from natural Moroccan clay: Application to filtration of solution containing dyes and salts. *Applied Clay Science*, **31**, 110–119.

Sahnoun, R.D. and Baklouti S. (2013) Characterization of flat ceramic membrane supports prepared with kaolin-phosphoric acid-starch. *Applied Clay Science*, **83–84**, 399–404.

Salahi, A., Gheshlaghi, A., Mohammadi, T., and Madaeni, S.S. (2010a) Experimental performance evaluation of polymeric membranes for treatment of an industrial oily wastewater. *Desalination*, **262**, 235–242.

Salahi, A., Abbasi, M., and Mohammadi, T. (2010b) Permeate flux decline during UF of oily wastewater: Experimental and modeling. *Desalination*, **251**, 153–160.

Scott, K., Adhamy, A., Atteck, W., and Davidson, C. (1994) Crossflow microfiltration of organic/water suspensions. *Water Research*, **28**, 137–145.

Scott, K., Jachuck, R.J., and Hall, D. (2001) Crossflow microfiltration of water-in-oil emulsions using corrugated membranes. *Separation and Purification Technology*, **22–23**, 431–441.

Shackelford, C.D. and Lee, J.M. (2003) The destructive role of diffusion on clay membrane behavior. *Clays and Clay Minerals*, **51**, 186–196.

Song, C., Wang, T., Pan, Y., and Qiu, J. (2006) Preparation of coal-based microfiltration carbon membrane and application in oily wastewater treatment. *Separation and Purification Technology*, **51**, 80–84.

Vasanth, D., Pugazhenthi, G., and Uppaluri, R. (2011a) Fabrication and properties of low cost ceramic microfiltration membranes for separation of oil and bacteria from its solution. *Journal of Membrane Science*, **379**, 154–163.

Vasanth, D., Uppaluri, R., and Pugazhenthi, G. (2011b) Influence of sintering temperature on the properties of porous ceramic support prepared by uniaxial dry compaction method using low-cost raw materials for membrane applications. *Separation Science and Technology*, **46**, 1241–1249.

Vasanth, D., Pugazhenthi, G., and Uppaluri, R. (2013) Cross-flow microfiltration of oil-in-water emulsions using low cost ceramic membranes. *Desalination*, **320**, 86–95.

Weir, M.R., Rutinduka, E., Detellier, C., Feng, C.Y., Wang, Q., Matsuura, T., and Mao, R. Le Van (2001) Fabrication, characterization and preliminary testing of all-inorganic ultrafiltration membranes composed entirely of a naturally occurring sepiolite clay mineral. *Journal of Membrane Science*, **182**, 41–50.

Zhang, Y., Jin, Z., Wang, Y., and Cui, P. (2010) Study on phosphorylated Zr-doped hybrid silicas/PSF composite membranes for treatment of wastewater containing oil. *Journal of Membrane Science*, **361**, 113–119.

Zhou, J., Chang, Q., Wang, Y., Wang, J., and Meng, G. (2010) Separation of stable oil–water emulsion by the hydrophilic nano-sized ZrO_2 modified Al_2O_3 microfiltration membrane. *Separation and Purification Technology*, **75**, 243–248.

(*Received 11 December 2014; revised 2 August 2015; Ms. 939; AE: P.B. Malla*)